Journal of Renewable Materials
DOI:10.32604/jrm.2020.09369
Article

Tech Science Press

Adsorption and Desorption Characteristics of Cadmium Ion by Ash-Free Biochars

Li Fu[1,2], Xianying Xu[1,2,*], Guiquan Fu[2], Renduo Zhang[3] and Hujun Liu[2]

[1]College of Forestry, Gansu Agricultural University, Lanzhou, 730070, China
[2]State Key Laboratory Breeding Base of Desertification and Aeolian Sand Disaster Combating, Gansu Desert Control Research Institute, Lanzhou, 730070, China
[3]Guangdong Provincial Key Laboratory of Environmental Pollution Control and Remediation Technology, Sun Yat-sen University, Guangzhou, 510006, China
*Corresponding Author: Xianying Xu. Email: xyingxu@163.com
Received: 07 December 2019; Accepted: 27 April 2020

Abstract: The aim of this study was to investigate adsorption and desorption characteristics of cadmium ion (Cd(II)) by ash-free biochars and the adsorption mechanism. Biochars were prepared using peanut shell, bamboo, and *Sophora japonica* Linn. Ash-free biochars were obtained by treating the biochars with acid elution. Adsorption and desorption data from batch experiments were analyzed using the Langmuir and Freundlich models and three adsorption kinetics models (i.e., the Pseudo second-order, Elovich model, and the Intraparticle diffusion models). Results showed that the acid elution improved the pore structure of biochars, increased C content and aromatic functional group content, enhanced biochars hydrophobicity and adsorption capacity for Cd(II). Ash-free peanut shell biochar showed the best Cd(II) adsorption performance among the biochars. Adsorption of ash-free peanut shell biochar reached the equilibrium within 6 h with adsorption capacity of 34.2 mg/g. The adsorption conditions were optimized by orthogonal experiment. The Cd(II) removal efficiency achieved 91.7% with the optimized condition: initial concentration of Cd(II) of 50 mg/L, pH of 5, adsorption time of 12 h, and temperature of 15°C. Isothermal adsorption of Cd(II) by the six biochars was best described with the Langmuir model, indicating that the adsorption was a physical-chemical composite process. The desorption isotherm showed the hysteresis between adsorption and desorption. The main mechanism of Cd(II) adsorption of the ash-free biochars was a complex interaction of physical and chemical reactions, mainly including electrostatic adsorption, cationic-π, and ligand exchange.

Keywords: Ash-free; biochars; Cd(II); adsorption; desorption

1 Introduction

The non-biodegradability and persistence of heavy metals make them a serious threat to the environment. Cadmium ion (Cd(II)) is a common heavy metal in wastewater. According to the national soil pollution survey data released by the Ministry of Environmental Protection in 2014, the exceeding

standard rate of cadmium reached the highest (i.e., 7.0%) among the studied heavy metals [1], which is listed as the first category of pollutants to be strictly controlled globally. The emission concentration of Cd(II) is an important index for environmental monitoring. In China's first-class standards of wastewater discharge, Cd (II) is stipulated as ≤ 0.1 mg/L [2]. Huang et al. [3] showed that Cd(II) in surface sediments of the main stream of Huangpu river was twice of the background value, and Cd(II) in Suzhou Creek exceeded the standard rate by 75%.

Adsorption is one of the efficient methods to remove heavy metals from the environment [4]. As an adsorbent, biochar is a refractory, highly aromatic and carbon-rich material produced by pyrolysis of biomass under complete or partial hypoxia [5–7]. Biochars used for heavy metal adsorption can be produced using straw [8–9], sludge [10–11], and animal manure [12]. The feedstock material composition determines the pore structure, surface properties, pH, and nutrient content of biochars, and these characteristics are the key factors affecting adsorption capacity. During the pyrolysis of biochar, many byproducts are produced, such as solid inorganic salts, liquid tar, and ash [13]. Ash on biochar surface mainly exists in the form of oxides or carbonates of mineral elements (e.g., Na, K, Mg, and Ca). Yuan et al. [14] showed that mineral elements and pH of biochar increased with the ash content, which affected the adsorption efficiency of biochar on organic matter. Abduiiah et al. [15] found that biochars produced from ash-rich biomass feedstock materials contained high ash content. Similarly, the ash content of biochars prepared with plants was lower than that with poultry manure [16,17]. Covering functional groups on biochar surface, ash greatly affects biochar adsorption. Metal oxides in ash also fill micropores of biochars, resulting in the decrease of specific surface area [18]. Tong et al. [19] and Jiang et al. [20] showed that a large number of cations (i.e., Na^+, K^+, Ca^{2+}, and Mg^{2+}) released from biochar competed with Cu^{2+} for adsorption sites, which was not conducive to the adsorption of Cu^{2+} by biochar. Since the cation content in the adsorption system of biochar after adsorption of heavy metal ions is higher than that before adsorption [21], the basic cations in the biochar ash can compete with the heavy metals in aqueous solution, thus reduce the adsorption capacity of the biochar for heavy metals [20]. Removal of the byproducts on biochar surface can effectively improve the adsorption capacity of biochar [22]. Zhang et al. [23] showed that ash removal increased the specific surface area of biochars as well as the adsorption capacity of carbaryl and atrazine. Guo et al. [20] reported that ash removal enhanced the adsorption capacity of biochar to copper ion.

With increasing shortage of resources, it is of great importance to recycle agricultural and forestry wastes. Peanut shell accounts for 30% of the total annual output of peanut (about 15 million tons), it mainly contains hemicellulose and cellulose, which reaches 68.7% of the total, accounting for about 75–80% of the dry weight of peanut shell [24]. The bamboo forest area in China is 5 million hm^2, accounting for 4% of the National forested area [25]. The *Sophora japonica* Linn. is widely used in landscaping, which produces huge amount of residue each year [26]. The cellulose and lignin content of wood materials (bamboo and *Sophora japonica* Linn.) is higher, and the ash content is relatively low [27]. Therefore, the objectives of this research were to utilize biochars produced using the agricultural and forestry residues as an adsorbent of Cd(II) in wastewater, and to study the adsorption characteristics of ash-free biochars as well as the adsorption mechanism.

2 Materials and Methods

2.1 Preparation and Acid Elution of Biochars

2.1.1 Preparation of Biochars

Biochars were produced using peanut shell, bamboo, and branches of *Sophora japonica* Linn. The feedstock materials were washed, dried, ground, sieved (by a 2 mm sieve), placed in an open muffle furnace (BLMT-1800B, Bolemante) with isolated oxygen at 500°C with a heating rate of 25 °C·min^{-1}, and continuously carbonized for 3 h. After the muffle furnace was naturally cooling down to room

temperature. The biochars produced from peanut shell, bamboo, and *Sophora japonica* Linn. were denoted as PBC, BBC, and GBC, respectively.

2.1.2 Acid Elution of Biochars

The biochars were repeatedly soaked in 1 mol L^{-1} HCl and HCl-HF solution (with a 1:1 volume ratio) to remove metal oxides and silica oxides on the biochar surface [23,28]. All the treatments were soaked in an oscillator (TS-110X50, Shanghai Tiancheng) at the solid-liquid ratio of 1:10 for 10 h. The supernatant was removed after being centrifuged for 20 min at 5000 r/min and repeated 4 times. The biochars were rinsed with deionized water until the conductivity of the eluate was < 10 μS/cm. Ash content of the biochars was measured after drying. The above acid elution steps were repeated until the ash in the biochars was completely removed. The ash-free biochars were denoted as A-PBC, A-BBC, and A-GBC, respectively.

2.2 Characterization of Biochars

The ash content was measured by combusting the biochars at 750°C for 6 h in an open crucible [29]. Contents of carbon (C), hydrogen (H) and nitrogen (N) of the biochars were measured using a CHN elemental analyzer (Vario EL III, Elementar). Oxygen content was estimated by mass difference (100%—% of C, H, N, and ash). Elemental composition was measured in triplicate, which were averaged [30,31]. FTIR spectra were collected in the range of 400~4000 cm^{-1} by Digilab FTS-3000, USA, with a resolution of 4 cm^{-1}. Biochar samples were ground in an agate mortar and then mixed with KBr at an mass ratio of 1:100, which then was pressed at 10 ton cm^{-2} for 3 min with a Perkin-Elmer hydraulic presser. The spectrum of a similar thickness KBr pellet was used as the background [30,31]. The shape and surface characteristics of samples were scanned using an electron microscope (TM4000 Plus, Hitachi, Japan) with the scanning voltage of 15.0 kV. Different magnification factors were used to adjust the visual field clarity, and the parts with complete structure were selected for analysis and preservation.

2.3 Batch Adsorption Studies

2.3.1 Kinetic Study

A batch equilibration method was used to study adsorption of Cd(II) onto adsorbents of A-PBC, PBC, A-BBC, BBC, A-GBC, and GBC. Time intervals of 0.25, 0.5, 1, 1.5, 2, 3, 6, 12, and 24 h were selected to investigate the time effect on Cd(II) adsorption onto the biochars. The initial concentration of Cd(II) in the solution was 80 mg/L, and the mass of each adsorbent was 0.1 g. The optimal pH of the solution was adjusted to 5.0. Kinetics solutions were agitated on a shaker at a 200 rpm and 25 ± 0.5°C. Mixtures were filtered with a 0.45 μm PTFE hydrophobic syringe filter (AlfaChem, Poland), then the filtrate was used for analyzing Cd(II) concentration with the atomic absorption spectrometry method (AAS) at 228.8 nm (Beijing East-West Analytical Instrument Co., Ltd.).

2.3.2 Adsorption-Desorption Isotherm Study

Adsorption capacity of Cd(II) onto the adsorbents were obtained according to the initial run of adsorption isotherm of Cd(II). The adsorption isotherms were carried out at an initial pH of 5.0 for Cd (II). Cd(II) concentrations ranging from 10 to 300 mg/L were used during the experiments. A single adsorption system consisted of 10 mL of solution and 0.1 g of biochars. Solutions were agitated on a shaker at a 200 rpm and 25 ± 0.5°C for 24 h. For desorption study, a desorptive agent of $NaNO_3$ with background electrolyte 2 mL was mixed with biochars with Cd(II) adsorbed on surface. The remaining steps were the same as the adsorption test. Three repeats were set up for each treatment.

2.3.3 Optimization of pH and Temperature

Following experiments were carried out to study impact of pH and temperature of solutions on Cd(II) adsorption onto the adsorbents. Cd(II) concentrations from 10 to 300 mg/L were used with pH of 5.0 and

each adsorbent mass of 0.1 g. The solutions were agitated on a shaker with temperatures of 15, 25, 35 ± 0.5°C for 24 h, respectively. In addition, initial pH values of solutions were adjusted to the range from 2 to 8 with Cd(II) concentration of 80 mg/L and each adsorbent mass of 0.1 g. The solutions were agitated on a shaker with 25 ± 0.5°C for 24 h.

2.4 Data Analysis

2.4.1 Adsorption Calculation

Cd(II) adsorbed on biochar was calculated for each sorbent as follows:

$$q_e = \frac{(C_0 - C_e)V}{1000m} \tag{1}$$

where q_e is the amount of adsorbed Cd(II) (mg/g); C_0 is the initial Cd(II) concentration (mg/L); C_e is Cd(II) concentration at the equilibrium (mg/L); V is Cd(II) solution volume (L); m is adsorbent weight (mg).

2.4.2 Adsorption Kinetic Study

The kinetics data were analyzed using the pseudo-second order kinetics (Eq. (2)), the Elovich equation (Eq. (3)), and the intra-particle diffusion equation (Eq. (4)):

$$\frac{t}{Q_t} = \frac{1}{k_2 Q_e{}^2} + \frac{t}{Q_t} \tag{2}$$

$$Q_t = a + b \ln t \tag{3}$$

$$Qt = k_p t^{0.5} + C \tag{4}$$

where k_2 and k_p are the quasi second-order rate constant (mg/(g/h)) and the intra-particle diffusion coefficient (mg/(g/h)), respectively; t is the reaction time (h); Q_t is the adsorption amount at time t and Q_e is the adsorption amount at the equilibrium of adsorption (mg/g); a is a constant that depends on the initial velocity of the reaction; b is a constant related to the adsorption activation energy (mg(g/h$^{-1/2}$)); C is a constant related to the boundary of adsorbent thickness.

2.4.3 Adsorption Isotherm Studies

The isotherm data were analyzed using the Freundlich (Eq. (5)) and Langmuir (Eq. (6)) models:

$$\lg q_e = \lg K_F + \left(\frac{1}{n}\right)\lg C_e \tag{5}$$

$$\frac{1}{q_e} = \frac{1}{Q_{\max}} + \left(\frac{1}{K_L Q_{\max}}\right)\left(\frac{1}{C_e}\right) \tag{6}$$

where q_e is the adsorption quantity at equilibrium (mg/g); K_F and n represent constants of adsorption capacity and favorable adsorption trend, respectively; C_e is the solution concentration at equilibrium (mg/L); $Q_{\max}$ is the maximum adsorption capacity of the metal ion per unit weight of sorbent (mg/g); K_L is the adsorption constant of the Langmuir model.

Hysteresis coefficient was estimated as follows:

$$HI = \frac{1/n_{des}}{1/n_{ads}} \tag{7}$$

where $1/n_{des}$ and $1/n_{ads}$ are the Freundlich constants of adsorption and desorption, respectively.

2.4.4 Gibbs Free Energy Equation

According to fitting parameter $\lg K_F$ from the Freundlich model, the Gibbs free energy equation was used to analyze the influence of temperature on the equilibrium adsorption coefficient by using the following equations:

$$\Delta G^\circ = -RT \ln K \tag{8}$$

$$\Delta G^\circ = \Delta H^\circ - T\Delta S^\circ \tag{9}$$

where ΔG° is the standard free energy change of ion exchange (J/mol); R is the universal gas constant (8.314 J/mol K); T is the absolute temperature (K); ΔH° is the enthalpy (kJ/mol); ΔS° is the entropy (J/mol K).

3 Results

3.1 Characterization of Biochars and Ash-Free Biochars

As shown in Tab. 1, the biochars were alkaline before acid elution with pH value increase with the ash content. Main elements in the biochars were C and O before acid elution, with the highest C content in PBC (61.5%) and the lowest in BBC (43.3%), and the O content between 34.8% and 53.2%. The contents of H and N among the biochars were similar, ranging from 1.83% to 2.89% and from 1.38% to 1.67%, respectively. The acid elution reduced the ash content to < 5% but increased the C content of biochars. The changing trend of N and H was consistent with that before acid elution, i.e., A-GBC > A-PBC > A-BBC. Biochars with lower values of O/C, H/C and (H+O)/C indicate the biochars with stronger hydrophobicity, more aromatic functional groups, and lower polarity, thus had stronger adsorption effect on pollutants [32]. Before acid elution, the C/N was the highest and the nitrogen content was the lowest in PBC. The lowest (O+H)/C in PBC indicated that PBC had greater polarity, stronger ion retention ability, and better adsorption performance. For the ash-free biochars, the lowest C/N ratio of A-GBC indicated the highest content of nitrogen oxides in A-GBC. The lowest H/C, O/C, and (O+H)/C values in A-PBC suggested that A-PBC had the highest aromatic functional group, stronger hydrophobicity, and lower polarity, thus had better adsorption performance. The adsorption characteristics of PBC and A-PBC may be attributable to the high content of hemicelluloses, cellulose, and carbon [24,33].

Table 1: Elemental composition and atomic ratios of peanut shell biochar (PBC), bamboo biochar (BBC), and *Sophora japonica* biochar (GBC), and ash-free biochars (A-PBC, A-BBC, and A-GBC)

Adsorbent	Mass percentage (%)				Ash (%)	Atomic ratio				pH
	C	H	N	O		H/C	C/N	O/C	(O+H)/C	
PBC	61.5	1.83	1.56	34.8	41.6	0.03	39.6	0.57	0.60	10.3
BBC	43.3	1.64	1.38	53.2	29.6	0.04	31.3	1.24	1.27	8.56
GBC	48.3	2.89	1.67	46.8	30.3	0.06	31.5	0.97	1.03	9.75
A-PBC	79.2	1.98	1.58	17.2	3.61	0.03	50.1	0.22	0.24	2.42
A-BBC	49.9	1.92	1.41	46.8	4.97	0.04	35.2	0.96	0.99	2.50
A-GBC	57.8	3.00	1.82	37.3	4.22	0.05	32.1	0.65	0.78	2.60

The SEM images showed that the acid elution procedure greatly influenced the surface morphology of the biochars (Fig. 1). PBC had long strip macropores on the surface, while A-PBC kept the surface structure with incresed surface pores and larger pore size. BBC had a lot of micropores, while for A-BBC some larger pore tunnels on the surface collapsed to form more smaller pores [34], thus the carbon surface became smoother. Similar to BBC, the surface pore morphology of GBC was honeycomb-like. In A-GBC, the

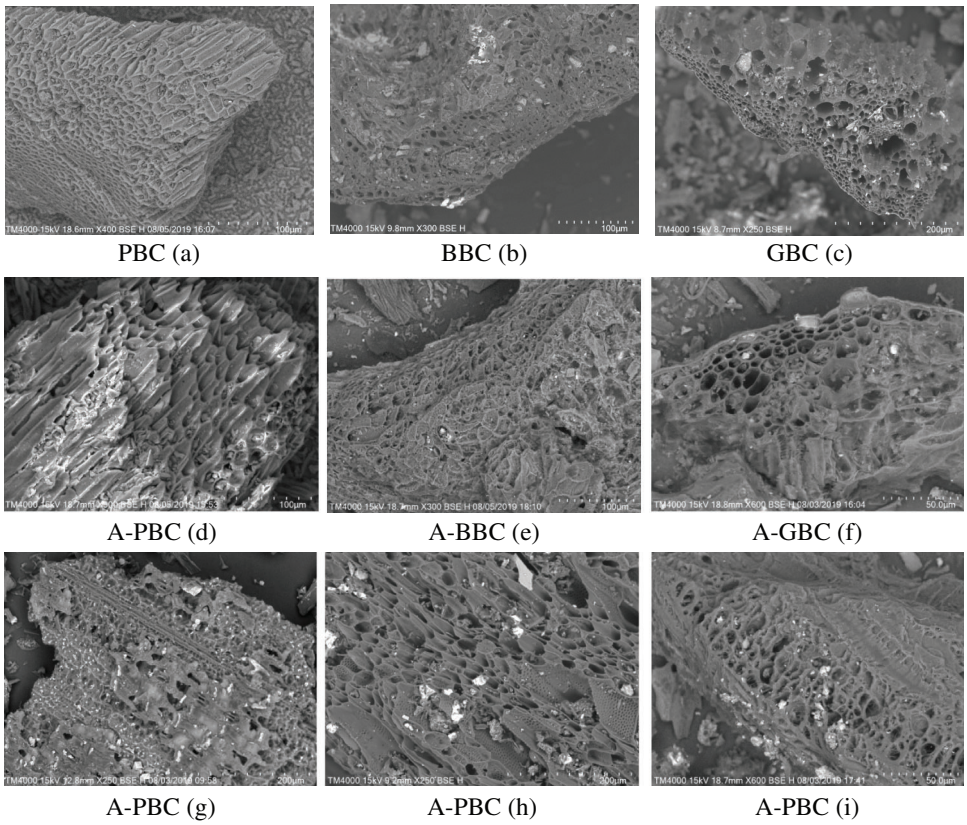

Figure 1: SEM images of peanut shell biochar (PBC) (a), bamboo biochar (BBC) (b), and *Sophora japonica* biochar (GBC) (c), ash-free biochars (A-PBC, A-BBC, and A-GBC) (d, e, f), and ash-free biochars with Cd (II) adsorption (g, h, i)

number of micropores on the surface increased and the size became larger. The formation of micropores in the biochars increased the specific surface area and adsorption capacity. Compared with BBC and GBC, the smoother surface of PBC indicated larger specific surface area and number of micropores, thus higher adsorption capacity. As shown in Figs. 1g–1i, the large number of particles on the surface indicated that the adsorption of Cd(II) mainly occurred on the surface of biochars [35]. The result was similar to Cheng et al. to study Cd(II) adsorption with peanut shell biochar [36].

3.2 FTIR Analysis

FTIR spectra of the six biochars are presented in Fig. 2. The wide and strong absorption peak band at 3400–3500 cm^{-1} was attributed to the stretching vibration of free or associated -OH. The strength of hydroxyl vibration peaks decreased after acid elution of the three biochars, indicating that the acid elution reduced the number of -COOH and -OH on the biochar surface, thus decreased alkalinity and hydrophilicity of the biochar. The strong absorption peak around 2900 cm^{-1} was attributed to the vibration of C-H functional groups in aldehydes. The vibration peak area in this range decreased after acid elution, indicating that the acid elution reduced the number of C-H bonds and removed byproducts on the biochar surface. The absorption peak at 1600–1700 cm^{-1} was related to the stretching vibration of aromatic (C=C) rings on C=O. The absorption peak at 1000–1200 cm^{-1} was attributed to the stretching vibration of C-O-C [37]. The peak intensity of PBC, BBC, and GBC decreased after acid elution, indicating that acid elution reduced the number of C-O-C groups on the biochar surface. After repeated acid eltion, the absorption peaks of Si-O-Si

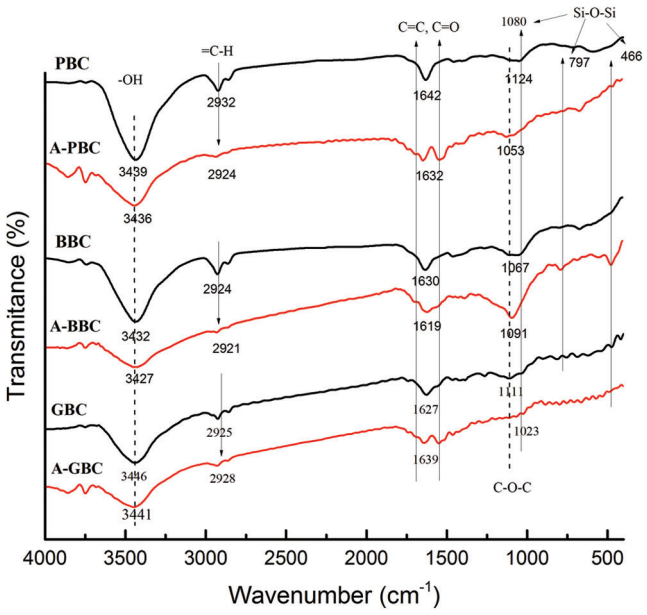

Figure 2: FTIR spectra of peanut shell biochar (PBC), bamboo biochar (BBC), and *Sophora japonica* biochar (GBC), and ash-free biochars (A-PBC, A-BBC, and A-GBC)

at 1081, 797, and 466 cm^{-1} were relatively weakened, and most of the inorganic minerals (e.g., SiO_2) on the biochar surface were removed. Therefore, the adsorption capacity of biochars to Cd(II) was improved. As shown by the FTIR spectra, the C-H aromatic functional groups, stable-OH functional groups, and C=C and C=O functional groups in the biochars suggested that π-π electron donor and receptor functions, electrostatic interaction, and hydrogen bonding might be the main mechanism of Cd(II) adsorption by biochars.

3.3 Adsorption Kinetics of Biochars and Ash-Free Biochars

Adsorption of Cd(II) by BBC, A-BBC, GBC, and A-GBC reached the equilibrium within 3 h and the equilibrium adsorption capacity was 2.66, 3.56, 2.51, and 3.32 mg/g, respectively. Adsorption of Cd(II) by PBC and A-PBC reached the equilibrium within 6 h and the equilibrium adsorption capacity was 6.14 and 7.80 mg/g, respectively (Fig. 3). The adsorption capacity was in the order of A-PBC > PBC > A-BBC > A-GBC > BBC > GBC. The experimental data of adsorption kinetics were fit with the quasi-second-order model, Elovich model, and the intraparticle diffusion model. As shown in Tab. 2 and Fig. 4, the quasi-second-order model was the best to describe the adsorption kinetics of Cd(II) by the six biochars with the coefficient of determination $R^2 > 0.94$, followed by the Elovich model with R^2 of 0.844–0.915, and the intraparticle diffusion model with $R^2 < 0.702$.

3.4 Adsorption-Desorption Isotherm of Biochars and Ash-Free Biochars

3.4.1 Adsorption Isotherm

With the increase of equilibrium concentrations of the solution, the adsorptive amount of Cd(II) by the biochars also increased (Fig. 5). Due to the different surface structure and properties of the biochars, the adsorptive capacity of the biochar to Cd(II) were significantly different and A-PBC had the highest adsorptive capacity to Cd(II). The equilibrium adsorption test data were fit with the Freundlich and Langmuir models (Fig. 6 and Tab. 3). Both models well fit the adsorption isotherm of Cd(II) by the six biochars. The Langmuir model is usually used to describe the monolayer adsorption, and Q_m is the maximum adsorption capacity of the monolayer. The adsorption of Cd(II) by PBC and A-PBC was larger than that of other biochars with Q_m values of 30.32 and 34.18 mg/g, respectively. The maximum

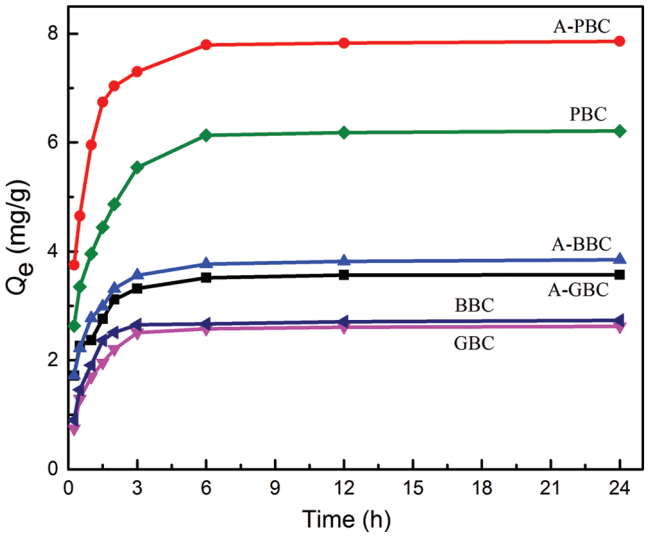

Figure 3: Kinetics of Cd(II) adsorption by peanut shell biochar (PBC), bamboo biochar (BBC), and *Sophora japonica* biochar (GBC), and ash-free biochars (A-PBC, A-BBC, and A-GBC)

Table 2: Fitting parameters for Cd(II) adsorption kinetics by peanut shell biochar (PBC), bamboo biochar (BBC), and *Sophora japonica* biochar (GBC), and ash-free biochars (A-PBC, A-BBC, and A-GBC)

Adsorbent	Pseudo-second-order model			Elovich model			Particle diffusion model		
	Q_e (mg/g)	k_2 (mg/(g/h))	R^2	a	b	R^2	K_p (mg/(g/h))	C	R^2
PBC	6.32	0.330	0.956	4.09	0.86	0.915	0.764	3.338	0.702
BBC	2.78	1.111	0.886	2.23	0.18	0.503	0.317	1.602	0.491
GBC	2.79	0.601	0.983	1.67	0.42	0.854	0.351	1.346	0.578
A-PBC	8.07	0.384	0.990	5.77	0.92	0.844	0.771	5.057	0.565
A-BBC	3.92	0.687	0.986	2.71	0.48	0.886	0.413	2.317	0.624
A-GBC	3.61	0.819	0.942	2.55	0.43	0.886	0.372	2.194	0.642

adsorption capacity of the six biochars to Cd(II) was in the order of A-PBC > PBC > A-GBC > A-BBC > BBC > GBC. The Freundlich model is suitable to describe inhomogeneous adsorption, in which lgK_F is the adsorption capacity of adsorbents. The increase of lgK_F in the ash-free biochars indicated that acid elution could enhance the adsorption capacity of biochars. The adsorption intensity (1/n) values of Cd(II) by the six biochars < 1 showed the L-type adsorption isotherm [38]. The lowest 1/n value of A-PBC indicated that A-PBC most easily to adsorb Cd(II), while the highest 1/n value of A-GBC indicated the most difficult adsorption of Cd(II).

3.4.2 Desorption Isotherm

Desorption isotherms of the six biochars are presented in Fig. 7. The great differences between the adsorption isotherms and desorption isotherms (Fig. 6 *vs.* Fig. 7) indicated that the adsorption and desorption processes were not reciprocal. The strong adsorption capacity of biochar enhances the desorption lag effect of pollutants. Microporous regulation effect is mainly attributable to microporous filling to cause desorption lag [39]. In the adsorption stage, small molecules enter into the interior of

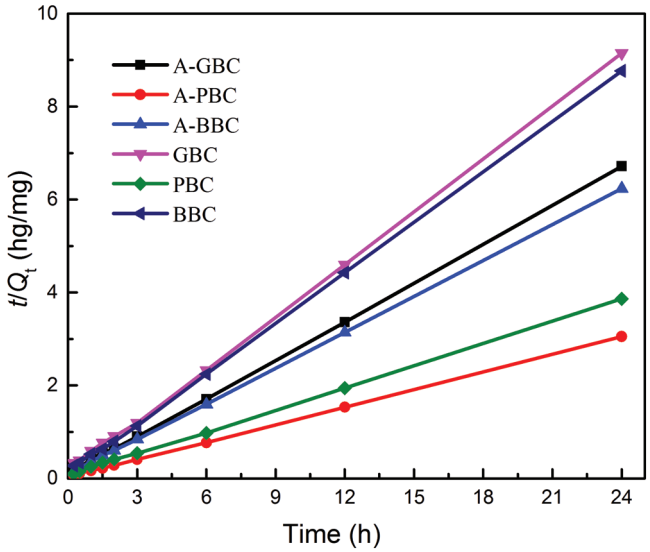

Figure 4: Fitting Cd(II) adsorption kinetics data of peanut shell biochar (PBC), bamboo biochar (BBC), and *Sophora japonica* biochar (GBC), and ash-free biochars (A-PBC, A-BBC, and A-GBC) with the Pseudo-second-order model

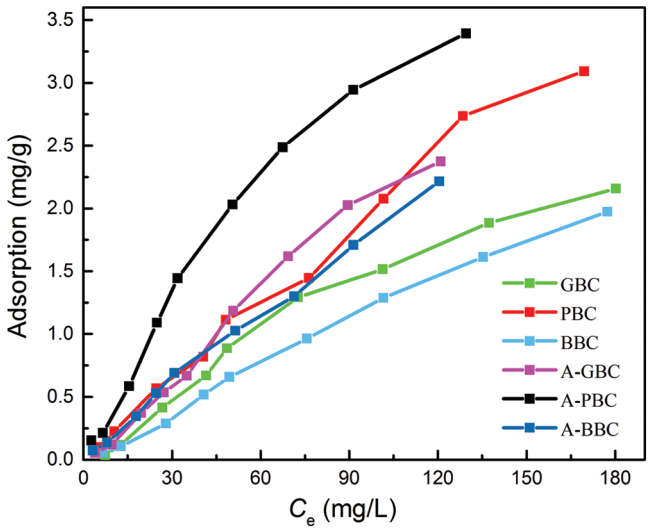

Figure 5: Isothermal adsorption of Cd(II) by peanut shell biochar (PBC), bamboo biochar (BBC), and *Sophora japonica* biochar (GBC), and ash-free biochars (A-PBC, A-BBC, and A-GBC)

biochar, resulting in changes of the shape and size of microporous structure. Cd(II) entered the micropores of biochar through adsorption, while Cd(II) was difficult to desorb from the micropore structure. The restoration of deformable micropores to the original shape produced hysteresis, resulting in that some Cd(II) could not be released [40,41].

The hysteresis coefficient (*HI*) (Eq. (7)) was introduced to describe the desorption behavior and the hysteresis effect. A *HI* value < 0.7 indicates that the adsorbate is not easily desorbed from the adsorbent (i.e., a positive hysteresis effect). A *HI* value in 0.7 < *HI* < 1 indicates no desorption hysteresis effect. A *HI* value > 1 indicates that the adsorbate is easily detached from the adsorbent (i.e., a negative hysteresis

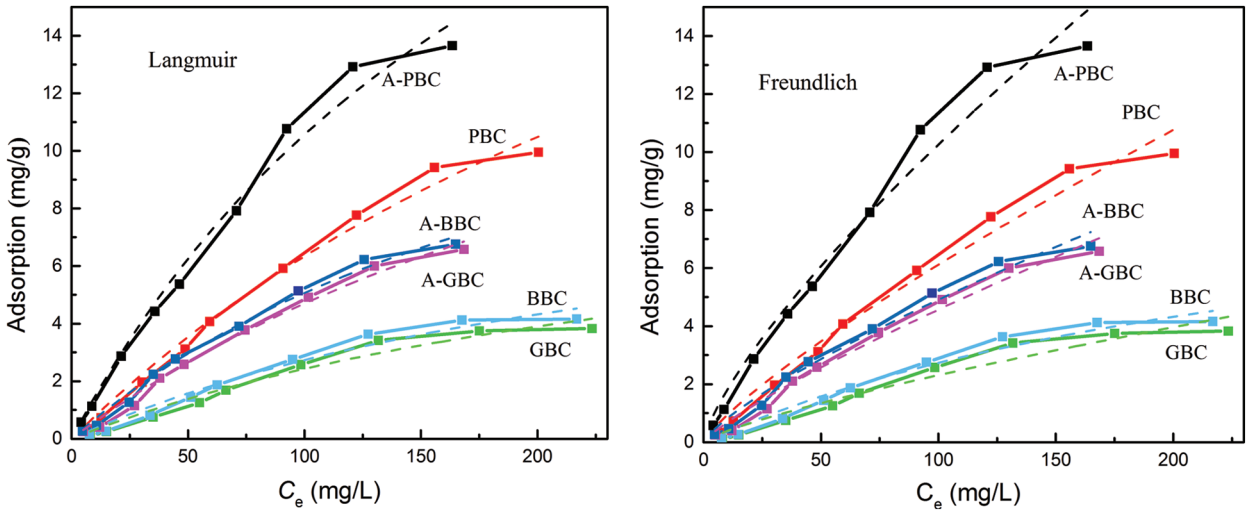

Figure 6: Curve fitting of Cd(II) adsorption by peanut shell biochar (PBC), bamboo biochar (BBC), and *Sophora japonica* biochar (GBC), and ash-free biochars (A-PBC, A-BBC, and A-GBC) with the Langmuir and Freundlich models

Table 3: The parameters for adsorption isotherm of Cd(II) by peanut shell biochar (PBC), bamboo biochar (BBC), and *Sophora japonica* biochar (GBC), and ash-free biochars (A-PBC, A-BBC, and A-GBC)

Adsorbent	Langmuir parameter			Freundlich parameter			*HI*
	K_L	Q_m (mg/g)	R^2	lgK_F	1/n	R^2	
PBC	0.0026	30.32	0.990	0.143	0.816	0.981	1.113
BBC	0.0036	10.29	0.972	0.077	0.765	0.953	1.204
GBC	0.0033	9.889	0.967	0.064	0.778	0.948	1.010
A-PBC	0.0045	34.19	0.987	0.313	0.758	0.976	1.078
A-BBC	0.0041	17.46	0.992	0.136	0.778	0.982	1.184
A-GBC	0.0030	20.63	0.991	0.101	0.827	0.983	1.163

effect) [42,43]. As shown in Tab. 3, the *HI* values > 1 suggested that Cd(II) had a negative hysteresis effect on the biochars. The desorption hysteresis might be attributable to the filled micropores and changes of micropore shape and size of the adsorbent [39]. Biochar adsorbed molecules through deformation of micropores in the adsorption process, while the micropores could not be quickly restored to the prototype in the desorption process.

3.5 Adsorption Thermodynamics of Biochars and Ash-Free Biochars

Isothermal adsorption of Cd(II) by PBC and A-PBC at different temperatures (i.e., 288, 298, and 308 K) is shown in Fig. 8. The adsorption capacity of A-PBC to Cd(II) increased with temperture. The Freundlich and Langmuir models well described the isothermal adsorption process of Cd(II) by the biochars at different temperatures (Tab. 4). The 1/n values < 1 indicated the L-type isothermal adsorption. The increase of lgK_F values with temperature suggested temperature enhancement of the adsorption capacity of the biochars to Cd (II). As shown in Tab. 5, the negative values of Gibbs free energy of Cd(II) on PBC and A-PBC at different temperatures indicated spontaneous adsorption processes. Since the ΔG° values were negative and their

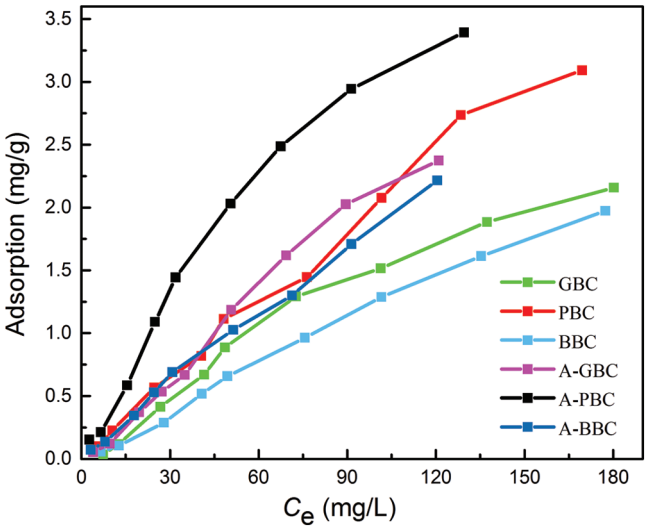

Figure 7: Isothermal desorption of Cd(II) by peanut shell biochar (PBC), bamboo biochar (BBC), and *Sophora japonica* biochar (GBC), and ash-free biochars (A-PBC, A-BBC, and A-GBC)

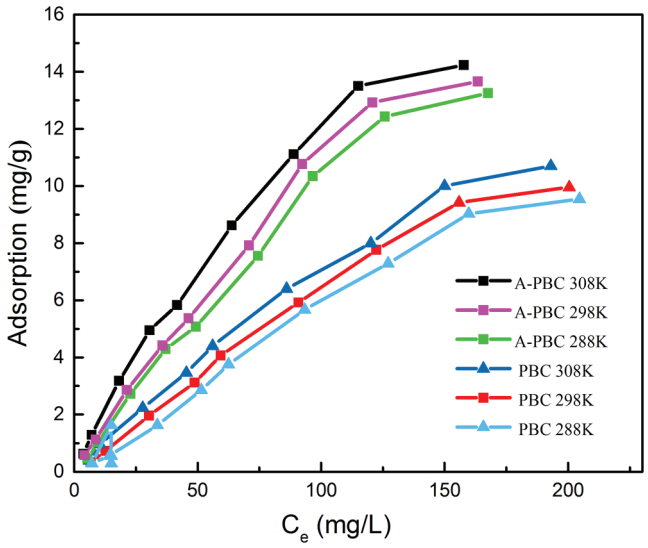

Figure 8: Isothermal adsorption of Cd(II) by peanut shell biochar (PBC) and ash-free biochar (A-PBC) at different temperatures (288, 298, 308 K)

absolute values < 40 kJ/mol, the adsorption of Cd(II) by the biochars should be dominated by physical adsorption [44]. The positive $\Delta H°$ values for the adsorption of Cd(II) by the biochars at different temperatures indicated endothermic reactions, that is, temperature increase enhanced the adsorption process [45]. At different temperatures, the positive $\Delta S°$ values of Cd(II) on the biochars indicated that the adsorption process increased entropy, i.e., the disorder of solid-liquid interface [46].

3.6 Effect of pH on Cd(II) Adsorption by Biochars and Ash-Free Biochars

With the adsorption time of 24 h, the removal rates of Cd(II) from PBC and A-PBC increased first then slightly decreased with the initial pH values of solutions. The removal rates of A-PBC were higher than those of PBC. At pH = 2, the removal rates of Cd(II) by PBC and A-PBC were 27.3% and 56.0%, respectively. At

Table 4: The parameters for adsorption models of Cd(II) by peanut shell biochar (PBC) and ash-free biochar (A-PBC)

Adsorbent	Temperature	Langmuir model			Freundlich model		
	(K)	K_L	Q_m (mg/g)	R^2	lgK_F	1/n	R^2
PBC	288	0.0017	39.48	0.981	0.091	0.892	0.975
	298	0.0026	30.32	0.990	0.143	0.816	0.981
	308	0.0033	28.77	0.995	0.187	0.781	0.988
A-PBC	288	0.0037	36.68	0.987	0.253	0.789	0.978
	298	0.0045	34.18	0.987	0.313	0.756	0.976
	308	0.0069	28.57	0.992	0.476	0.688	0.981

Table 5: Thermodynamic parameters for the adsorption of Cd(II) by peanut shell biochar (PBC) and ash-free biochar (A-PBC)

Adsorbent	$\Delta G°$ (J/mol)			$\Delta H°$ (J/mol)	$\Delta S°$ (J/mol K)
	288 K	298 K	308 K		
PBC	–0.502	–0.816	–1.103	8.148	0.0301
A-PBC	–1.395	–1.786	–2.807	19.04	0.0706

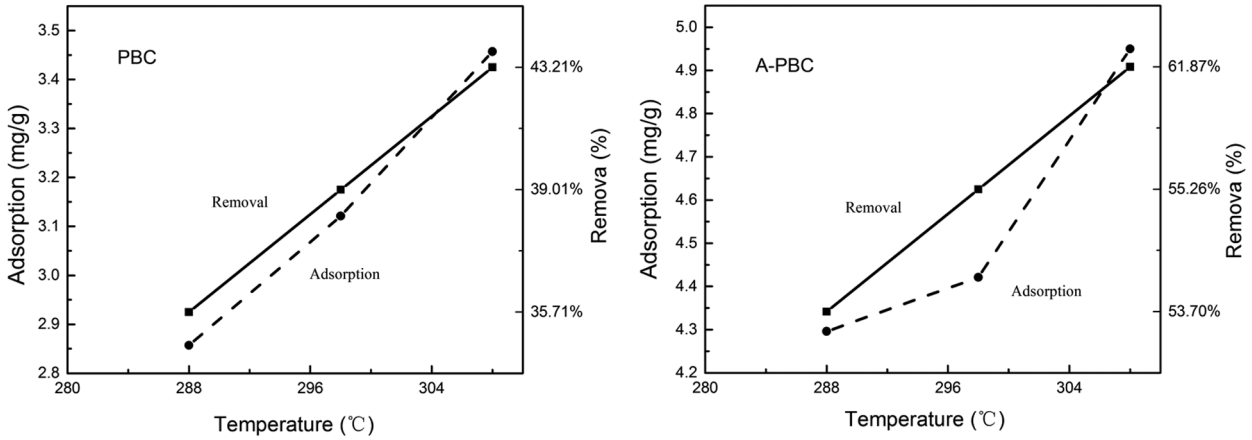

Figure 9: Adsorption capacity of Cd(II) on peanut shell biochar (PBC), and ash-free biochar (A-PBC) at different temperatures

pH = 5, the removal rates by PBC and A-PBC reached the highest values of 75.2% and 95.8%, respectively. At pH > 6, the removal rates became stable. The change of pH affects the morphology of heavy metals and the ionization state of some functional groups on the adsorbent surface to varying degrees [47]. At lower pH, the competitive adsorption of Cd(II) and H^+ on the surface of biochar hindered the approaching of Cd(II). In addition, due to pH < pH_{pzc}, the biochar surface was positively charged and mutually repelled with Cd(II) in the solution [48]. With pH increase, the negative charge on biochar surface increases [49], and more binding sites are released. At the same time, the organic functional groups (e.g., -COOH and -OH) on the surface react with Cd(II) to form surface complexes. Therefore, the acid dissociation degree of organic functional

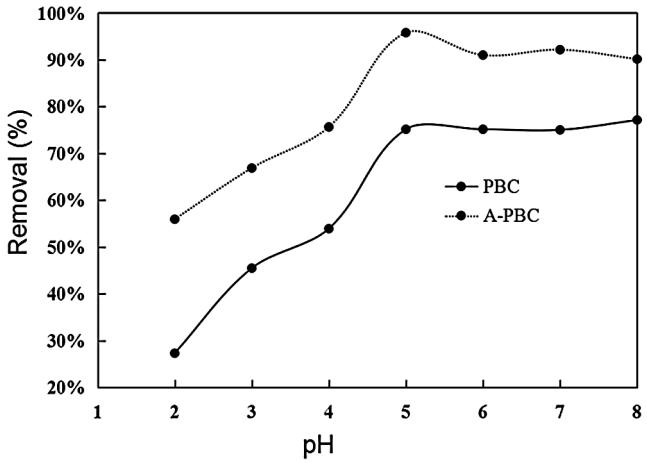

Figure 10: Adsorption of Cd(II) by peanut shell biochar (PBC), and ash-free biochar (A-PBC) in solutions with different pH values

groups increases, and the complexing ability with Cd(II) is enhanced, which increases the adsorption amount and the removal rate [50]. With further increase of pH, Cd(II) presented in the form of $CdOH^+$ and $Cd(OH)_2$, and Cd(II) and OH^- precipitated, which reduced the removal rate of Cd(II) by biochar [51]. In this test, with the relatively low initial concentration of Cd(II) (i.e., 80 mg/L), the Cd(II) was further hydrolyzed and continuously adsorbed to the active sites of biochar with pH increase.

3.7 Orthogonal Experiment

A L9 orthogonal experiment was designed to determine the optimal adsorption conditions of Cd(II) by A-PBC and the influence of each factor on the removal rate. In the experiment, factors included adsorption time, solution pH value, temperature, and initial concentration, three levels were selected for each factor. The best conditions for the adsorption of Cd(II) by A-PBC are shown in Tab. 6.

The optimal combination of Cd(II) adsorption by A-PBC was $A_3B_2C_1D_1$ (Tab. 6). Under of the optimized adsorption condition of the initial concentration of Cd(II) of 50 mg L^{-1}, pH of 5, adsorption time of 12 h, and temperature of 15°C, the Cd(II) removal efficiency achieved 91.7%. The influence on the removal rate of the four factors was in the order of pH > adsorption time > initial concentration > temperature.

4 Discussion

4.1 Adsorption Kinetics of Cd(II) on Biochars

The adsorption of Cd(II) by biochars can be divided into three stages of rapid increase, slow increase, and final equilibrium. In the initial stage of adsorption, biochar has a strong adsorption capacity with many available adsorption sites on the biochar surface. With continuous adsorption reaction, adsorption sites on the surface of biochar are occupied continuously, leading to decrease of adsorption rate [52]. When all adsorption sites are saturated, the adsorption reaction reaches the equilibrium state [53]. Cd(II) may also diffuse into biochar pores and further reacts with the internal active sites, which is a relatively slow adsorption process and not significant [54]. To ensure complete adsorption, an adsorption time of 24 h was chosen for all the adsorption tests in this study. Compared with other biochars, A-PBC had the largest adsorption capacity because the acid elution did not destroy the regular pore structure of PBC, but increased the number and size of surface pores.

Table 6: Orthogonal experimental results

No.	Adsorption time (h)	Solution pH	Temperature (°C)	Initial concentration (mg/L)	Removal rate (%)
1	1 (3)	1 (4)	1 (15)	1 (50)	51.0
2	1	2 (5)	2 (25)	2 (80)	91.3
3	1	3 (6)	3 (35)	3 (100)	38.8
4	2 (6)	1	1	1	43.9
5	2	2	2	2	97.4
6	2	3	3	3	52.3
7	3 (12)	1	1	1	56.5
8	3	2	2	2	97.8
9	3	3	3	3	64.3
k_1	57.0	50.0	67.0	70.9	
k_2	64.5	95.5	66.5	66.7	
k_3	72.9	48.4	60.9	56.9	
R	15.8	47.1	6.12	14.1	
Better level	A_3	B_2	C_1	D_1	

The good fitting results of the quasi-second-order kinetic model indicated that the adsorption of Cd(II) by biochars was a combination of chemical adsorption and physical diffusion. The smallest kinetic rate constant k_2 of A-PBC among the biochars (i.e., 0.3835 mg/(g/h)) indicated the longest time needed to reach adsorption equilibrium, which was attributed to the more adsorption sites for continuous adsorption of Cd(II). The fitting results with the models showed that the adsorption of Cd(II) by biochars involved many processes, including surface chemical deposition, electrostatic adsorption, and internal micropore diffusion. The non-zero C values in the particle diffusion model suggested that the particle diffusion process in the adsorption of Cd(II) by biochars was not significant to affect the adsorption rate. The adsorption process and characteristics (e.g., O/C, H/C and (H+O)/C) of PBC and A-PBC were significantly different from those of BBC, A-BBC, GBC and A-GBC. The result showed that the element composition, polarity, and hydrophobicity of biochars had a great influence on the adsorption characteristics of Cd(II).

4.2 Adsorption Isotherm of Cd(II) on Biochars

Adsorption isotherm is an important index to evaluate the interaction mechanism between adsorbate and adsorbent. The adsorption isotherms are rapidly first and then slowly, which is mainly due to the influence of adsorption site and adsorption process [55]. It can be explained that the initial concentration of the solution is low, the adsorbent can provide sufficient adsorption sites and active groups, while with the increase of the initial concentration of the solution, the adsorption sites gradually saturate, the active groups reduce, and the adsorbent reaches the saturation. Liu et al. [56] reported that the maximum adsorption capacity of peanut shell biochar to Cd(II) was 6.29 mg/g, which was similar to the maximum adsorption capacity of PBC in this study. Chen et al. [57] suggested that the maximum adsorption capacity of wastewater sludge biochar to Cd(II) was 42.80 mg/g. The large difference in adsorption amount among the biochars was related to the structure and physicochemical characteristics of biochars, mainly including the aromatic structure and oxygen-containing functional groups (e.g., -OH, -COO-, -O-) of biochar as well as cation-π

and ion exchange between biochar and heavy metals. In addition, for ash-free biochar, the acid elution increased specific surface area, opened blocked pores of biochars, and removed ash on the biochar surface to exposure organic surface and more pores, which provided more adsorption sites [58]. The Langmuir and Freundlich models well described the adsorption isotherm of Cd(II) by the six biochars. In this study, the concentrations of Cd(II) from 10 to 300 mg/L was the suitable range for application of the Freundlich model. The adsorption capacity order (i.e., A-PBC > PBC > A-BBC > A-GBC > BBC > GBC) was consistent with the equilibrium adsorption capacity of adsorption kinetics. The highest adsorption capacity of A-PBC was related to its loose structure, large specific surface area, better pore structure and more oxygen-containing functional groups.

4.3 Adsorption Thermodynamics of Cd(II) on Biochars

Temperature has an important influence on the adsorption of heavy metals in biochar. The adsorption of Cd(II) by the peanut shell biochar increased with temperature. The heterogeneous surface of PBC made the surface Gibbs free energy of some locations be very high with strong activity, which was prone to adsorption reaction. In addition increasing temperature could increase the amount of negative charges on the biochar surface and promote partial solution solubility of biochar, thus increase adsorption capacity of biochar. Increasing temperature also enhances the solubility of organic matter, accelerates the thermal movement of molecules in solution, increases the probability of their entry into the pore of adsorbent, thereby increases the adsorption capacity [59]. According to the Gibbs free energy, physical adsorption was the predominant process in the adsorption of Cd(II) by biochar, and the adsorption was a spontaneously endothermic reaction and increased entropy of the system.

5 Conclusions

Ash removal from biochar with acid elutuion increased adsorption sites and pores on the biochar surface, thus enhanced the adsorptive capacity of biochar for Cd(II). The adsorption equilibrium of A-PBC reached within 6 h with adsorption capacity of 34.2 mg/g. The Cd(II) removal efficiency achieved 91.7% under the optimized condition of initial concentration of Cd(II) of 50 mg/L, pH of 5, adsorption time of 12 h, and temperature of 15°C.

Isothermal adsorption of Cd(II) by the six biochars was well described with the Langmuir isotherm model and the desorption isotherm indicated hysteresis between adsorption and desorption. The adsorption kinetics data of Cd(II) by the biochars were best fit uisng the pseudo-second order model, indicating that the adsorption was a physical-chemical composite process.

The dominant mechanism of Cd(II) adsorption by the biochars included the presence of -OH functional groups and some C=C and C=O functional groups. Therefore, electrostatic adsorption, cationic-π and ligand exchange might be the main mechanism of Cd(II) adsorption by biochars.

Funding Statement: This project was supported by the Key Laboratory of Environmental Pollution Control and Restoration Technology of Guangdong province (2018K06), and the project was supported by the Major Science and Technology Projects of Gansu Province (18ZD2FA009), and a National key research and development plan (2018YFC0507102).

Conflicts of Interest: The authors declare that they have no conflicts of interest to report regarding the present study.

References

1. Chen, N. C., Zhen, Y. J., He, X. F., Li, X. F., Zhang, X. X. (2014). National soil pollution survey bulletin. *China Environmental Protection Industry, 5,* 10–11. DOI 10.11654/jaes.2017-1220.
2. Zhou, B. S. (2002). *Industrial Water Treatment Technology.* Beijing: Chemical Industry Press.

3. Huang, H. T., Liang, Y. P., Wei, C. C., Lin, H., Mo, G. L. (2009). Current situation of heavy metal pollution in water and its treatment technology. *Guangxi Journal of Light Industry, 25(5),* 99–100. DOI 10.3969/j.issn.1003-2673.2009.05.053.
4. Demirbas, A. (2008). Heavy metal adsorption onto agro-based waste materials: a review. *Journal of Hazardous Materials, 157(2-3),* 220–229. DOI 10.1016/j.jhazmat.2008.01.024.
5. Zimmerman, A. R. (2010). Abiotic and microbial oxidation of laboratory-produced black carbon (biochar). *Environmental Science & Technology, 44(4),* 1295–1301. DOI 10.1021/es903140c.
6. Lehmann, J., Gaunt, J., Rondon, M. (2006). Bio-char sequestration in terrestrial ecosystems—a review. *Mitigation & Adaptation Strategies for Global Change, 11(2),* 403–427. DOI 10.1007/s11027-005-9006-5.
7. Chun, Y., Sheng, G., Chiou, C. T., Xing, B. (2004). Compositions and sorptive properties of crop residue-derived chars. *Environmental Science & Technology, 38(17),* 4649–4655. DOI 10.1021/es035034w.
8. Ahmad, M., Lee, S. S., Dou, X., Mohan, D., Sung, J-K. et al. (2012). Effects of pyrolysis temperature on soybean stover and peanut shell-derived biochar properties and TCE adsorption in water. *Bioresource Technology, 118,* 536–544. DOI 10.1016/j.biortech.2012.05.042.
9. Huang, H., Wang, Y. X., Tang, J. C., Zhu, W. Y. (2014). Properties of maize stalk biochar produced under different pyrolysis temperatures and its sorption capability to naphthalene. *Environmental Science, 35(5),* 1884–1890. DOI 10.13227/j.hjkx.2014.05.036.
10. Chen, T., Zhou, Z., Xu, S., Wang, H., Lu, W. et al. (2015). Adsorption behavior comparison of trivalent and hexavalent chromium on biochar derived from municipal sludge. *Bioresource Technology, 190,* 388–394. DOI 10.1016/j.biortech.2015.04.115.
11. Zhang W., Mao S., Chen H., Huang L., Qiu R. (2013). Pb(II) and Cr(VI) sorption by biochars pyrolyzed from the municipal wastewater sludge under different heating conditions. *Bioresource Technology, 147,* 545–552. DOI 10.1016/j.biortech.2013.08.082.
12. Song, W. P., Guo, M. X. (2012). Quality variations of poultry litter biochar generated at different pyrolysis temperatures. *Journal of Analytical & Applied Pyrolysis, 94(3),* 138–145. DOI 10.1016/j.jaap.2011.11.018.
13. Farrell, M., Macdonald, L. M., Baldock, J. A. (2015). Biochar differentially affects the cycling and partitioning of low molecular weight carbon in contrasting soils. *Soil Biology and Biochemistry, 80,* 79–88. DOI 10.1016/j.soilbio.2014.09.018.
14. Yuan, J. H., Xu, R. K., Zhang, H. (2011). The forms of alkalis in the biochar produced from crop residues at different temperatures. *Bioresource Technology, 102(3),* 3488–3497. DOI 10.1016/j.biortech.2010.11.018.
15. Abdullah, H., Wu, H. W. (2009). Biochar as a fuel: properties and grind ability of biochars produced from the pyrolysis of mallee wood under slow-heating conditions. *Energy & Fuels, 23(8),* 4174–4181. DOI 10.1021/ef900494t.
16. Shinogi, Y., Yoshida, H., Koizumi, T., Yamaoka, M., Saito, T. (2003). Basic characteristics of low-temperature carbon products from waste sludge. *Advances in Environmental Research, 7(3),* 661–665. DOI 10.1016/S1093-0191(02)00040-0.
17. Singh, B., Singh, B. P., Cowie, A. L. (2010). Characterisation and evaluation of biochars for their application as a soil amendment. *Australian Journal of Soil Research, 48(7),* 516–525. DOI 10.1071/SR10058.
18. Yuan, J. H., Xu, R. K. (2010). The amelioration effects of low temperature biochar generated from nine crop residues on an acidic ultisol. *Soil Use and Management, 27(1),* 110–115. DOI 10.1111/j.1475-2743.2010.00317.x.
19. Tong, X-J., Li, J-Y., Yuan, J-H., Xu, R-K. (2011). Adsorption of Cu(II) by biochars generated from three crop straws. *Chemical Engineering Journal, 172(2-3),* 828–834. DOI 10.1016/j.cej.2011.06.069.
20. Jiang, J., Peng, Y., Yuan, M., Hong, Z., Wang, D. et al. (2015). Rice straw-derived biochar properties and functions as Cu(II) and cyromazine sorbents as influenced by pyrolysis temperature. *Pedosphere, 2015(5),* 781–789. DOI 10.1016/S1002-0160(15)30059-X.
21. Wang, Z., Liu, G., Zheng, H., Li, F., Ngo, H. H. et al. (2015). Investigating the mechanisms of biochar's removal of lead from solution. *Bioresource Technology, 177,* 308–317. DOI 10.1016/j.biortech.2014.11.077.

22. Guo, Y., Tang, W., Dai, J. Y., Hu, L. C., Zhu, Q. T., et al. (2014). Influence of elution of biochar on its adsorption of Cu(II). *Journal of Agro-Environment Science, 33(7),* 1407–1413. DOI 10.11654/jaes.2014.07.022.
23. Zhang, P., Sun, H., Yu, L., Sun, T. (2013). Adsorption and catalytic hydrolysis of carbaryl and atrazine on pig manure-derived biochars: impact of structural properties of biochars. *Journal of Hazardous Materials, 244-245,* 217–224. DOI 10.1016/j.jhazmat.2012.11.046.
24. Zhou, R. B. (2003). *Peanut Processing Technology.* Beijing: Chemical Industry Press.
25. Zhang, Q. S., Jiang, S. H. (2002). Pay attention to the chemical utilization of bamboo and develop the application technology of bamboo charcoal. *Journal of Nanjing Forestry University (Natural Science Edition), 26(1),* 1–4. DOI 10.3969/j.issn.1000-6567.2001.03.006.
26. Zhao, W. N. (2018). *Production of biochar from urban greenwaste and its efficacy in adsorption of Pb^{2+} in aqueous solution*. Zhenjiang A & F University. Zhe Jiang, China.
27. Xu, Y. L. (2013). *Thermodynamic properties of biochar preparation sorption characteristics and mechanisms of cadmium onto biochars*. Zhejiang University. Zhe Jiang, China.
28. Zhou, F., Szczech, J., Pettes, M. T., Moore, A. L., Jin, S. et al. (2009). Characteristics of biochar: microchemical properties. *Journal of the Party School of Shengli Oilfield, 7(6),* 1649–1654. DOI 10.1021/nl0706143.
29. Chen, Z. M., Chen, B. L., Zhou, D. D. (2013). Composition and sorption properties of rice-straw derived biochars. *Journal of Environmental Science, 33(1),* 9–19. DOI 10.13671/j.hjkxxb.2013.01.005.
30. Qian, K., Kumar, A., Zhang, H., Bellmer, D., Huhnke, R. (2015). Recent advances in utilization of biochar. *Renewable and Sustainable Energy Reviews, 42(1),* 1055–1064. DOI 10.1016/j.rser.2014.10.074.
31. Rombolà, A. G., Meredith, W., Snape, C. E., Baronti, S., Genesio, L. et al. (2015). Fate of soil organic carbon and polycyclic aromatic hydrocarbons in a vineyard soil treated with biochar. *Environmental Science & Technology, 49 (18),* 11037–11059. DOI 10.1021/acs.est.5b02562.
32. Liao, P., Yuan, S., Xie, W., Zhang, W., Tong, M. et al. (2013). Adsorption of nitrogen-heterocyclic compounds on bamboo charcoal: kinetics, thermodynamics, and microwave regeneration. *Journal of Colloid and Interface Science, 390(1),* 189–195. DOI 10.1016/j.jcis.2012.09.037.
33. Yang, L., Xie, Y., Qiu, X. H., You, M. L. (2009). Studies on waste dye water processing with active peanut shell carbon. *Journal of Peanut Science, 38(1),* 10–17. DOI 10.14001/j.issn.1002-4093.2009.01.001.
34. Li, R. N., Wang, Z. W., Guo, J. L., Zhao, X. T., Li, Y., et al. (2017). Adsorption characteristics of sulfathiazole in aqueous solution by acid/alkali modified biochars. *Acta Scientiae Circumstantiae, 37(11),* 4119–4128. DOI 10.13671/j.hjkxxb.2017.0155.
35. Qiu Y., Cheng H., Xu C., Sheng G. D. (2008). Surface characteristics of crop-residuederived black carbon and lead (II) adsorption. *Water Research, 42(3),* 567–574. DOI 10.1016/j.watres.2007.07.051.
36. Cheng, Q. M., Huang, Q., Liu, Y. J., Liao, Z. N. (2014). Adsorption of cadmium ions by peanut and peanut biochar. *Journal of Agro-Environment Science, 33(10),* 2022–2029. DOI 10.11654/jaes.2014.10.020.
37. Wang, W. P., Chai, A. L., Shi, Y. X., Xie, X. W., Li, B. J. (2015). Quantitative detection of Chinese cabbage cluroot based on FTIR spectroscopy. *Spectroscopy and Spectral Analysis, 35(5),* 1243–1247. DOI 10.3964/j.issn.1000-0593(2015)05-1243-05.
38. Fröhlich, D. R., Amayri, S., Drebert, J., Reich, T. (2012). Influence of temperature and background electrolyte on the sorption of neptunium(V) on opalinus clay. *Applied Clay Science, 69(69),* 43–49. DOI 10.1016/j.clay.2012.08.004.
39. Braida, W. J., Pignatello, J. J., Lu, Y., Ravikovitch, P. I., Neimark, A. V. et al. (2003). Sorption hysteresis of benzene in charcoal particles. *Environmental Science & Technology, 37(2),* 409–417. DOI 10.1021/es020660z.
40. Lu, H. L., Zeng, X. Z., Ding, J. X., Tan, Y. Q. (2013). Remediation strategy on farmland soil polluted by heavy metal and organism. *Anhui Agricultural Science, 26,* 10633–10636. DOI 10.13989/j.cnki.0517-6611.2013.26.029.
41. Zhang, X., Wang, H., He, L., Lu, K., Sarmah, A. et al. (2013). Using biochar for remediation of soils contaminated with heavy metals and organic pollutants. *Environmental Science and Pollution Research International, 20(12),* 8472–8483. DOI 10.1007/s11356-013-1659-0.

42. Cox, L., Koskinen, W. C., Yen, P. Y. (1997). Sorption-desorption of imidacloprid and its metabolites in soils. *Journal of Agricultural & Food Chemistry, 45(4),* 1468–1472. DOI 10.1021/jf960514a.
43. Doretto, K. M., Peruchi, L. M., Rath, S. (2014). Sorption and desorption of sulfadimethoxine, sulfaquinoxaline and sulfamethazine antimicrobials in Brazilian soils. *Science of the Total Environment, 476-477,* 406–414. DOI 10.1016/j.scitotenv.2014.01.024.
44. Ying, B., Lin, G. L., Jin, L. S., Zhao, Y. T., Wang, J. G. (2015). Effect of corn cob biochar on the adsorption of 2,4-Dichlorophenoxyacetic acid in spiked soil. *Acta Scientiae Circumstantiae, 35(5),* 1491–1497. DOI 10.13671/j.hjkxxb.2014.0845.
45. Andreae, M. O., Merlet, P. (2001). Emission of trace gases and aerosols from biomass burning. *Global Biogeo Chemical Cycles, 15(4),* 955–966. DOI 10.1029/2000GB001382.
46. Zhang, Z. L., Kuang, Q., Jia, X. S. (2010). Study on kinetics and thermodynamics of adsorption of Pb^{2+}, Cu^{2+}, Cr^{3+}, Cd^{2+} and Ni^{2+} from peanut shell. *Ecology and Environmental Sciences, 19(12),* 2973–2977. DOI 10.3969/j.issn.1674-5906.2010.12.035.
47. Sari, A., Tuzen, M. (2009). Removal of Mercury(II) from aqueous solution using moss (*Drepanocladus revolvens*) biomass: equilibrium, thermodynamic and kinetic studies. *Journal of Hazardous Materials, 171(1–3),* 500–507. DOI 10.1016/j.jhazmat.2009.06.023.
48. Goel, J., Kadirvelu, K., Rajagopal, C. (2004). Mercury(II) removal from water by coconut shell based activated carbon: batch and column studies. *Environmental Technology, 25(2),* 141–153. DOI 10.1080/09593330409355447.
49. Tong, X. J., Li, J. Y., Jiang, J., Xu, R. K. (2011). Effect of biochars derived from crop straws on Cu(II) adsorption by red soils. *Journal of Ecology and Rural Environment, 27(5),* 37–41. DOI 10.3969/j.issn.1673-4831.2011.05.007.
50. Li, R. Y., Chen, D., Li, L. Q., Pan, G. X., Chen, J. Q. (2015). Adsorption of Pb(II) and Cd(II) in aqueous solution by biochars derived from different crop residue. *Journal of Agro-Environment Science, 34(5),* 1001–1008. DOI 10.11654/jaes.2015.05.025.
51. Ozacar, M., Sengil, I. A. (2003). Adsorption of reactive dyes on calcined alunite from aqueous solutions. *Journal of Hazardous Materials, 98(1-3),* 211–224. DOI 10.1016/S0304-3894(02)00358-8.
52. Wang, G. Z., Tao, J. H., Li, L. H., Yu, J. T., Xu, M. (2015). Study of adsorption of nitrate nitrogen in water on biomass charcoals derived from different pyrolysis temperatures and sources. *Science Technology and Engineering, 15(6),* 109–113. DOI 10.3969/j.issn.1671-1815.2015.06.022.
53. Aslam, M., Rais, S., Alam, M., Pugazhendi, A. (2013). Adsorption of Hg(II) from aqueous solution using Adulsa (*Justicia adhatoda*) leaves powder: kinetic and equilibrium studies. *Journal of Chemistry, 2,* 295–316. DOI 10.1155/2013/174807.
54. Wu, C., Zhang, X., Li, G. (2007). Sorption of Hg^{2+}, As^{3+}, Pb^{2+} and Cd^{2+} by black carbon. *Journal of Agro-Environment Science, 26(2),* 70–774. DOI 10.3321/j.issn:1672-2043.2007.02.070.
55. Wang, T. T., Ma, J. B., Qu, D., Zhang, X. Y., Zheng, J. Y., et al. (2017). Characteristics and mechanism of copper adsorption from aqueous solutions on biochar produced from sawdust and apple branch. *Environmental Science, 38(5),* 2161–2171. DOI 10.13227/j.hjkx.201610124.
56. Liu, Y. Y., Qin, H. Z., Li, L. Q., Pan, G. X., Zhang, X. H. (2012). Adsorption of Cd(II) and Pb(II) in aqueous solution by biochars produced from the pyrolysis of different crop feedstock. *Ecology and Environmental Sciences, 21(1),* 146–152. DOI CNKI:SUN:TRYJ.0.2012-01-027.
57. Chen, T., Zhou, Z., Han, R., Meng, R., Wang, H. et al. (2015). Adsorpion of cadmium by biochar derived from municipal sewage sludge: impact factors and adsorption mechanism. *Chemosphere, 134,* 286–293. DOI 10.1016/j.chemosphere.2015.04.052.
58. Oh T. K., Choi B., Shinogi Y., Chikushi J. (2012). Effect of pH conditions on actual and apparent fluoride adsorption by biochar in aqueous phase. *Water Air & Soil Pollution, 223(7),* 3729–3738. DOI 10.1007/s11270-012-1144-2.
59. Huang, P., Yue, L., Yu, H. M., Luo, J. W., Ge, C. J. (2018). Adsorption and desorption behavior of avermectin on biochar prepared by cassava residue. *Chinese Journal of Tropical Crop, 39(2),* 361–371. DOI 10.3969/j.issn.1000-2561.2018.02.023.